

## Dirac point in the photon dispersion relation of a negative/zero/positive-index plasmonic metamaterial

Vassilios Yannopapas\* and Alexandros Vanakaras

*Department of Materials Science, University of Patras, GR-26504 Patras, Greece*

(Received 14 December 2010; revised manuscript received 28 April 2011; published 19 July 2011)

We report on the emergence of a Dirac point in the dispersion relation of a plasmonic metamaterial. It is realized as a three-dimensional crystal (cubic or orthorhombic) whose lattice sites are decorated by aggregates of gold nanoparticles embedded in a high-index dielectric material. The Dirac-type dispersion lines of the photon modes are not a result of diffraction as in photonic crystals but due to subwavelength features and emerge from the gapless transition from a negative to a positive index band. The Dirac point is manifested as a dip in the spectrum of light transmittance through a finite slab of the metamaterial; however, transmittance does not decrease diffusively but exponentially due to the inherent losses of gold in the given spectral regime.

DOI: [10.1103/PhysRevB.84.045128](https://doi.org/10.1103/PhysRevB.84.045128)

PACS number(s): 42.70.Qs, 42.25.Bs, 42.50.Gy, 78.67.Pt

One of the salient features of graphene, i.e., a monolayer of carbon atoms that occupy the sites of a honeycomb lattice<sup>1</sup> is the presence of conical singularities in the electron band structure, i.e., conically shaped valleys touching each other at the corners of the Brillouin zone. These singularities are known as Dirac points since the energy dispersion relation around these points reduces to the Dirac equation of a massless relativistic particle.<sup>2,3</sup> Photonic and phononic crystals possessing triangular symmetry are the electromagnetic (EM) and elastic counterparts of graphene, respectively. Under certain conditions, they can exhibit Dirac singularities in the frequency band structure as has been numerically predicted<sup>4,5</sup> and experimentally verified in sonic<sup>6</sup> and microwave experiments.<sup>7</sup> The opening of the Dirac singularity (gap creation) in honeycomb photonic crystals by time-reversal-symmetry breaking can lead to one-way defect-free waveguiding of light with important applications in optoelectronics.<sup>8</sup> Dirac points in the band structure of ultracold atoms trapped in honeycomb optical lattices have also been reported.<sup>9</sup>

Dirac singularities in the band structure have been reported for two-dimensional (2D) honeycomb<sup>4,5</sup> or square lattices.<sup>8,10</sup> There, the Dirac singularity appears at an edge of the Brillouin zone and, as such, corresponds to both finite frequency  $\omega$  and wave vector  $k$ . However, it has been recently suggested that a Dirac point can emerge at the center of the Brillouin zone in a so-called negative-zero-positive (NZP) metamaterial, a material without a gap between a negative and a positive refractive-index band.<sup>11</sup> Metamaterials are artificial electromagnetic structures whose basic properties (artificial magnetism,<sup>14</sup> negative effective index,<sup>15</sup> near-field amplification,<sup>16</sup> cloaking,<sup>17</sup> perfect absorption,<sup>18</sup> etc.), unlike photonic crystals, are generally observed in the long-wavelength limit and are, therefore, characterized as subwavelength structures. A Dirac singularity of a metamaterial can also be a *subwavelength* feature and, as such, it will occur at the center of the Brillouin zone while in photonic crystals, it is a result of wave *diffraction*. NZP metamaterials based on transmission lines<sup>12</sup> and split-ring resonator/wire technology<sup>13</sup> have been realized in the GHz regime.

In this work, we report on the emergence of a Dirac singularity in the dispersion relation of a three-dimensional (3D) plasmonic NZP metamaterial in the optical regime.

Namely, the metamaterial under study is a orthorhombic lattice whose sites are occupied by aggregates of metallic nanoparticles (NPs) embedded in a dielectric host (see Fig. 1). Originally, this type of metamaterial has been proposed as a candidate structure possessing a dispersive permeability in the optical regime via the excitation of strong Mie resonances of the EM field within a single cluster of metallic NPs.<sup>19</sup> As shown below, for a dielectric surrounding with a sufficient large permittivity, such a metamaterial exhibits anomalous dispersion for the dominating eigenmode, i.e., increasing frequency with decreasing wavevector within a certain spectral region. The latter, however, potentially suggests negative refraction only for materials with low losses where wave propagation is meaningful.<sup>20</sup> Unfortunately, this does not hold in the present example. Nevertheless, for sufficiently high dielectric constant of the material surrounding the NPs of the cluster, the real part of the dispersion relation of the metamaterial may exhibit a continuous (gapless) transition from a negative to a positive refractive index giving rise to a Dirac singularity. The refractive index herein is defined as the norm of the real part of the propagation constant of the lowest order Bloch mode normalized to the length of the wavenumber in free space. The Dirac singularity manifests itself here as a distinct minimum in the transmission spectrum of light incident on a finite slab of the metamaterial over a narrow frequency domain.

As stated above, the basic unit which repeats itself in the metamaterial is a cluster of 100 nonoverlapping metallic NPs, namely, gold NPs embedded in an insulating host of dielectric constant  $\epsilon$  (see Fig. 1). The positions of the gold particles within the aggregates are taken from a Monte-Carlo simulation of the self-organization of these particles under a spherically confining potential. All particles have the same radius  $S = 8.8$  nm while the average radius of the cluster is  $S_c = 42.67$  nm. The dielectric function of a single gold NP is taken from experiment<sup>21</sup> with corrections accounting for finite-size effects [see Eqs. (3) and (4) of Ref. 22]. In order to study the optical response of a single cluster of NPs, we have employed an EM direct-space multiple-scattering method for an arbitrary collection of a finite number of scatterers.<sup>23</sup> Based on this method, we have calculated the scattering cross section of light incident on the above cluster where the spheres

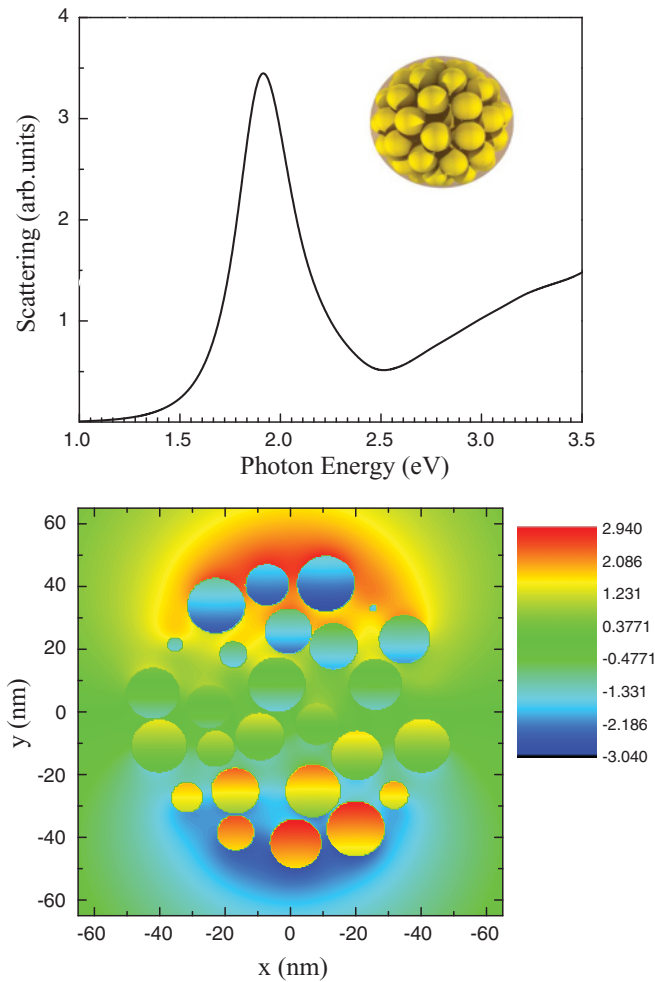


FIG. 1. (Color online) (Upper panel) Scattering cross section of light incident on the spherical cluster shown in the inset. The cluster consists of 100 nonoverlapping gold nanoparticles of radius  $S = 8.8$  nm in a nearly close-packed arrangement with cluster radius 42.67 nm. (Lower panel)  $z$ -component of the scattered magnetic field generated by a  $z$ -propagating and  $x$ -polarized plane wave illuminating the cluster of the figure at the peak frequency (1.9 eV) of the scattering cross section. The field is plotted within the  $xy$ -plane which is an equatorial cross section of the cluster.

are assumed to be embedded in a dielectric with  $\epsilon = 5$ ; see Fig. 1. For definiteness, the incident field propagates along the  $z$ -direction and its electric field is polarized along the  $x$ -direction (the particular choice of the polarization direction is of marginal importance due to the spherical symmetry of the particle). It is evident that scattering exhibits a prominent peak at about 1.9 eV which is lower than the energy of 2.05 eV corresponding to the dipolar surface plasmon (SP) resonance of an isolated gold NP embedded in a host medium with  $\epsilon = 5$ . A similar redshift of the SP resonance has been reported for clusters of gold nanospheres embedded in an aqueous medium.<sup>24,25</sup> At the same time, the clusters also exhibit a significant magnetic activity as manifested in the nontrivial variation of the effective magnetic permeability for a medium made of such clusters.<sup>25</sup> In order to confirm the magnetic activity in our case, we show, in the lower panel of Fig. 1, the  $z$ -component of the scattered magnetic field at an

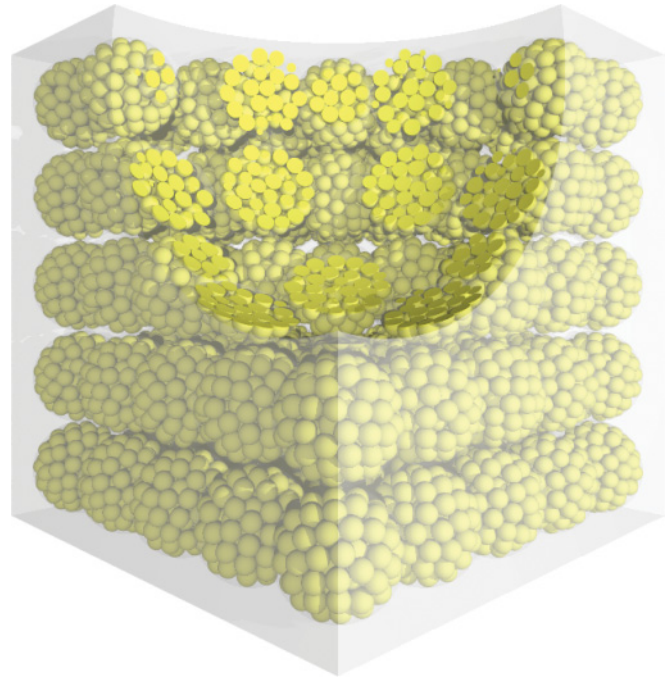


FIG. 2. (Color online) Quarter-spherical intersection of a 3D metamaterial made of the clusters of NPs of the inset of Fig. 1.

intersection ( $xy$ -plane) of the cluster of Fig. 1. The frequency of the illuminating plane wave corresponds to the the peak energy (1.9 eV) of the scattering cross section of the top panel of Fig. 1. It can be seen that the variation of the scattered magnetic field resembles a magnetic dipole (opposite values of the field at the two opposite poles of the spherical cluster). It is also worth noting that the magnetic field within the spheres is opposite to the one outside the spheres. The electric-field response is the one expected for metals for frequencies far below the plasma frequency which results in a strong electric response of the cluster. The significant magnetic activity along with the ordinary electric response of the cluster of NPs is a sign for a possible appearance of nontrivial variation of the refractive index (spectral regions of negative values) in a metamaterial consisting of the above clusters of NPs.

The metamaterial we have in mind is a slightly elongated cubic (orthorhombic) lattice viewed as a succession of 2D square lattices of the above clusters of gold NPs, parallel to the  $xy$ -plane (see Fig. 2). The lattice constant of the 2D square lattice is  $a_x = a_y = 85.22$  nm while the lattice constant in the  $z$ -direction is  $a_z = 87.86$  nm. It is essential that the choice of lattice and corresponding parameters is more or less arbitrary since the metamaterial under study is a *par excellence* subwavelength structure where the details of the underlying lattice are not crucial. In order to study the EM response of such a metamaterial, we have employed a two-stage multiple-scattering method for light. At the first stage, we employ the direct-space EM multiple-scattering method described above<sup>23</sup> in order to calculate the scattering  $T$ -matrix of the *entire* cluster.<sup>26</sup> The latter is embedded within an existing layer-multiple-scattering formalism and computer code<sup>27</sup> which provides the transmission, reflection, and absorption coefficients of an EM wave incident on a slab consisting of a number of layers which can be either planes

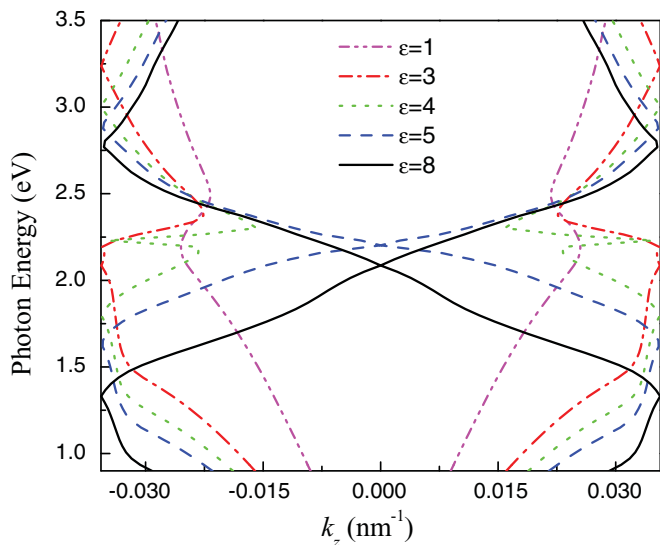


FIG. 3. (Color online) Real part of the dispersion relation for the lowest order Bloch eigenmode,  $\omega = \omega(k'_z)$ , at the center of the SBZ ( $\mathbf{k}_{\parallel} = \mathbf{0}$ ) for the orthorhombic ( $a_x = a_y = 85.22$  nm,  $a_z = 87.86$  nm) NZP metamaterial of Fig. 2 for different values of the dielectric constant  $\epsilon$  of the host medium surrounding the gold nanospheres.

of single particles or clusters of such particles (as in our case) with the same 2D periodicity. Apart from the above quantities, by imposing periodic boundary conditions into the third dimension, one can also obtain the (complex) frequency band structure of an infinite periodic crystal.<sup>27</sup>

Figure 3 shows the real part of the frequency band structure  $\omega = \omega(k'_z)$  of the above metamaterial for different host media surrounding the clusters (and the NPs within the cluster). We note that  $k_z$  is the  $z$ -component of the Bloch wave vector which is normal to the surface Brillouin zone (SBZ) of the 2D square lattice and it is generally a complex quantity, i.e.,  $k_z = k'_z + ik''_z$ . We recall that the other component of the Bloch wave vector, i.e.,  $\mathbf{k}_{\parallel}$  which is parallel to the SBZ and assumes values within it, is held fixed for a given band diagram such as the one shown in Fig. 3. In our case, we have chosen the center of the SBZ ( $\bar{\Gamma}$ -point), i.e.,  $\mathbf{k}_{\parallel} = \mathbf{0}$ . It is evident that, as the dielectric constant  $\epsilon$  of the host medium increases, we witness the formation of a Dirac singularity around 2.2 eV. When calculating the band structure in the layer-multiple-scattering method, one writes the EM field as a sum of plane waves and thus involves an infinite summation over the reciprocal-lattice vectors  $\mathbf{g}$  corresponding to a given 2D lattice (square in our case).<sup>27</sup> The band diagrams of Fig. 3 converge solely by the contribution of the field components corresponding to the reciprocal-lattice vector  $\mathbf{g} = \mathbf{0}$ . This means that the occurrence of the Dirac singularities in Fig. 3 is a subwavelength feature and other diffraction-generated components corresponding to vectors  $\mathbf{g} \neq \mathbf{0}$  are irrelevant. This also means that one can attach an effective refractive index  $n_{\text{eff}}$  to the band diagrams of Fig. 3: below the Dirac singularity,  $n_{\text{eff}}$  has a negative real part while above it, the real part of  $n_{\text{eff}}$  assumes positive values. The fact that the Dirac points emerge with increasing  $\epsilon$  of the host medium is attributed to the corresponding increasing strength of the magnetic and electric interactions among the NPs in a cluster (or among the clusters in the metamaterial) driven by

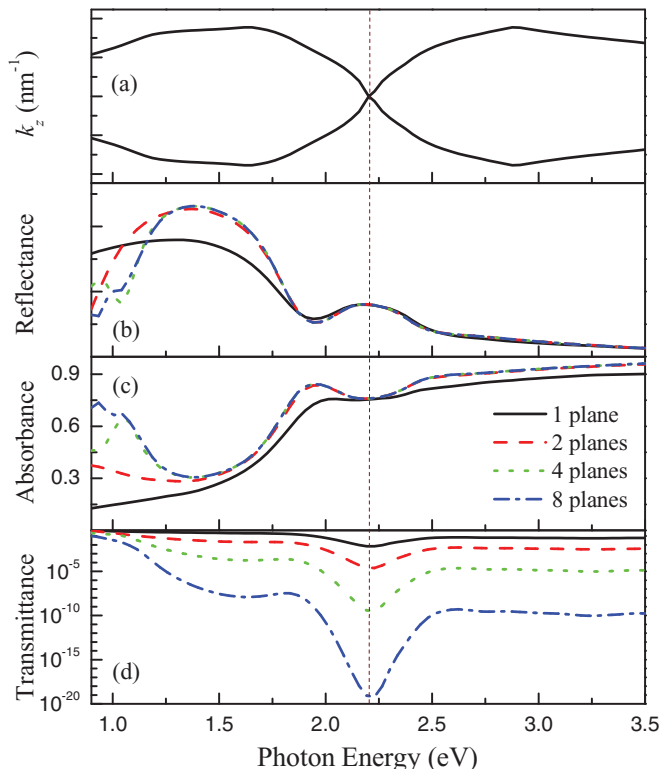


FIG. 4. (Color online) (a) Real frequency band structure,  $\omega = \omega(k'_z)$ , at the center of the SBZ ( $\mathbf{k}_{\parallel} = \mathbf{0}$ ) for the orthorhombic ( $a_{xy} = 85.22$  nm,  $a_z = 87.86$  nm) NZP metamaterial of Fig. 2 where the nanospheres are embedded in a host with  $\epsilon = 5$ . Reflectance (b), absorbance (c), and transmittance (d) of light incident normally on a finite slab of the NZP metamaterial of Fig. 2 consisting of different numbers of planes.

the increasing inductive and capacitive coupling among NPs (or clusters).

Figure 4(a) shows the band structure for  $\epsilon = 5$  (also shown in Fig. 3) along with the corresponding transmittance/reflectance and absorbance spectra for light incident normally ( $\mathbf{k}_{\parallel} = \mathbf{0}$ ) on finite slabs of the metamaterial of various thicknesses (number of planes). Evidently, at the frequency of the Dirac point, transmittance and absorbance exhibit a local minimum while reflectance exhibits a local maximum. A minimum in the transmittance at the Dirac singularity is also reported in lossless photonic crystals<sup>4-7</sup> in which case transmittance decreases linearly with the slab thickness (diffusive transport). In our case, however, from Fig. 4(d), it is evident that transmittance decreases exponentially with the number of planes due to the inherent losses of the gold NPs. Despite the losses, the response of a finite slab of the metamaterial under study is still governed by the Dirac equation. Since we study the case of normal incidence ( $\mathbf{g} = \mathbf{0}$ ) in the subwavelength regime (the contribution of the  $\mathbf{g} \neq \mathbf{0}$  components is negligible), wave propagation/attenuation within the slab is effectively described by the one-dimensional (1D) Dirac equation,

$$\begin{pmatrix} 0 & -iv_D \partial_x \\ -iv_D \partial_x & 0 \end{pmatrix} \begin{pmatrix} \psi_1 \\ \psi_2 \end{pmatrix} = (\omega - \omega_D) \begin{pmatrix} \psi_1 \\ \psi_2 \end{pmatrix}, \quad (1)$$

where  $\psi = (\psi_1, \psi_2)$  represents the amplitudes of the two EM modes corresponding to the two branches (with negative and positive propagations, respectively) of the dispersion relation around the Dirac point.  $\omega_D$  is the Dirac-point frequency and  $v_D$  is the corresponding Dirac velocity which is complex, in our case, in order to accommodate the losses of the metamaterial. The EM field outside the slab is described by the Helmholtz equation. Following the same procedure as in Ref. 4, it can be easily proven that the transmission coefficient is simply  $t = \exp(ik_z L)$ , where  $L$  is the slab thickness and  $k_z$  is the wave vector within the slab. The latter is a complex quantity, i.e.,  $k_z = k'_z + ik''_z$  in which case the transmittance is given by  $T = |t|^2 = \exp(-2k''_z L)$ . Therefore, given the transmittance spectrum  $T$ , one can calculate the imaginary part  $k''_z = -\ln T/(2L)$ . The latter is depicted by the dashed lines of Fig. 5. In the same figure, we also show  $k''_z$  (dotted lines) and  $k'_z$  (solid lines) as obtained by the complex frequency-band-structure solver of the LMS method [the dispersion lines for  $k'_z$  are the same as in Fig. 4(a)]. It can be seen that the  $k''_z$  found based on the Dirac equation and the one obtained by the rigorous LMS method are in a very good agreement which confirms the validity of the Dirac equation to describe the light propagation through the the metamaterial of Fig. 2. The constant offset is likely attributed to the impedance mismatch between the free space modes and the eigenmodes as sustained by the metamaterial. It will cause some spurious reflection which is not considered in the simplifying model.

We further investigated the presence of the Dirac singularity away from the center of the SBZ, i.e., for  $\mathbf{k}_{\parallel} \neq \mathbf{0}$ . Evidently, the Dirac singularity is lifted and at  $\omega_D$ , the wave vector assumes a finite value above and below the Dirac point. Therefore, around the center of the SBZ ( $\bar{\Gamma}$ -point), an isofrequency surface will have a conical shape similar to graphene. We have also confirmed the existence of a Dirac point in the dispersion

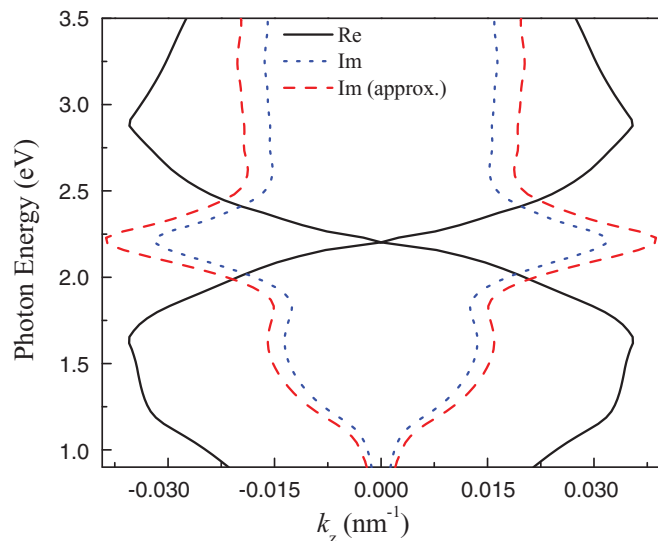


FIG. 5. (Color online) Complex frequency band structure,  $\omega = \omega(k'_z)$  and  $\omega = \omega(k''_z)$ , at the center of the SBZ ( $\mathbf{k}_{\parallel} = \mathbf{0}$ ) for the orthorhombic ( $a_{x,y} = 85.22$  nm,  $a_z = 87.86$  nm) NZP metamaterial of Fig. 2 where the nanospheres are embedded in a host with  $\epsilon = 5$ . The dashed lines are obtained by considering the metamaterial slab as an effective 1D Dirac medium governed by Eq. (1).

relation of an fcc metamaterial viewed as a succession of (001) planes of clusters (they are the same planes as those of the orthorhombic metamaterial of Figs. 2–5). The Dirac point occurs at about the same frequency as the orthorhombic one [Figs. 4(a) and 5]. Only the curvatures of the positive-index branch (above the Dirac point) of the dispersion lines differ substantially from the orthorhombic case.

A note on the possible realization of the NZP metamaterial under study. 1D and 2D lattices decorated by clusters of metallic NPs have already been realized by template-assisted colloidal self-organization. Namely, clusters of metallic NPs have been deposited within the voids of a 2D periodically perforated dielectric slab<sup>28</sup> or within the trenches of a 1D grating.<sup>29</sup> The resulting structures exhibited strong artificial magnetic response similarly to the present NZP metamaterial. Since the latter is a 3D structure, a template-assisted colloidal self-assembly should be applied to 3D dielectrics with spherical voids such as inverted opals. The latter are fcc photonic crystals of air holes in a dielectric host such as  $\text{SiO}_2$ ,  $\text{TiO}_2$ , or  $\text{Si}$ .<sup>30</sup> By infiltrating the air holes first with gold NPs and then by the dielectric host, one can realize the metamaterial of Fig. 2. Alternatively, a bottom-up self-assembly technique without the need of a (lithographically fabricated) template can be employed.<sup>24,25</sup> Namely, highly stable gold NPs are synthesized by the Turkey-Frens method<sup>31</sup> which are dispersed within an aqueous solution. By adding a ligand molecule within the solution, the NPs start to agglomerate into supramolecular clusters.<sup>24</sup> The nontrivial artificial magnetic activity demonstrated in these clusters<sup>25</sup> allows us to expect that a subsequent crystallization of the above solution can materialize the structure of Fig. 2.

The characterization of the structure based on the presence of the Dirac point can be conducted as follows. When a Dirac point occurs in the dispersion relation of a lossless crystal (e.g., dielectric photonic crystal), right at the Dirac frequency, an incident plane wave propagates diffusively within a finite slab of the crystal (transmittance is inversely proportional to the slab thickness). If such a behavior is observed experimentally for a finite slab of an *ordered* crystal and at a given frequency, the latter corresponds to a Dirac point. In our case, due to the inherent losses in the metallic nanoparticles, the transmittance as a function of slab thickness does not obey a power law (as it is the case for a Dirac point in a lossless system) but obeys an exponential decay. However, the same exponential decay is true for a crystal with a frequency band gap and, as such, one cannot distinguish between a Dirac singularity and a small band gap. It is therefore important to find an alternative route to verify the existence of a Dirac point in the plasmonic metamaterial under study. Due to the subwavelength nature of the structure (working wavelength much larger than the lattice period), one can measure the spectrum of the (complex) effective refractive index by spectroscopic ellipsometry. Right at the Dirac frequency, the real part of the effective refractive index should be zero while above (below) the Dirac frequency, it should be negative (positive). Another possibility is to infer the presence of a Dirac point *indirectly*. A good agreement between the theoretical and experimental reflectance spectra for various parameters of light incidence (angle of incidence, polarization) would imply that the fabricated structure is

a true realization of the theoretically proposed structure. However, this possibility is less robust than the spectroscopic ellipsometry mentioned above.

In conclusion, we have shown that it is possible to realize conical (Dirac) singularities in the photon dispersion relation by a 3D negative-zero-positive metamaterial consisting of spherical aggregates of gold NPs surrounded by a high-permittivity dielectric. The Dirac singularity is a subwavelength feature and as such it does not depend on the lattice type of the metamaterial. Despite the intrinsic losses of gold,

wave propagation/attenuation within the metamaterial can be described by a 1D Dirac equation for massless relativistic particles with a general complex velocity.

The research leading to these results has received funding from the European Union's Seven Framework Programme (FP7/2007-2013) under Grant Agreement No. 228455-NANOGOLD (Self-organized nanomaterials for tailored optical and electrical properties). V.Y. would like to thank Dr. Rockstuhl for critical reading of the manuscript.

\*vyannop@upatras.gr

<sup>1</sup>K. S. Novoselov, A. K. Geim, S. V. Morozov, D. Jiang, Y. Zhang, S. V. Dubonos, I. V. Grigorieva, and A. A. Firsov, *Science* **306**, 666 (2004).

<sup>2</sup>P. R. Wallace, *Phys. Rev.* **71**, 622 (1947).

<sup>3</sup>G. W. Semenoff, *Phys. Rev. Lett.* **53**, 2449 (1984).

<sup>4</sup>R. A. Sepkhanov, Ya. B. Bazaliy, and C. W. J. Beenakker, *Phys. Rev. A* **75**, 063813 (2007).

<sup>5</sup>X. Zhang, *Phys. Lett. A* **372**, 3512 (2008); *Phys. Rev. Lett.* **100**, 113903 (2008).

<sup>6</sup>X. Zhang and Z. Liu, *Phys. Rev. Lett.* **101**, 264303 (2008).

<sup>7</sup>S. R. Zandbergen and M. J. A. de Dood, *Phys. Rev. Lett.* **104**, 043903 (2010); S. Bittner, B. Dietz, M. Miski-Oglu, P. Oriá Iriarte, A. Richter, and F. Schäfer, *Phys. Rev. B* **82**, 014301 (2010); U. Kuhl, S. Barkhofen, T. Tudorovskiy, H. J. Stöckmann, T. Hossain, L. de Forges de Parney, and F. Mortessagne, *ibid.* **82**, 094308 (2010).

<sup>8</sup>F. D. M. Haldane and S. Raghu, *Phys. Rev. Lett.* **100**, 013904 (2008); *Phys. Rev. A* **78**, 033834 (2008); Z. Wang, Y. D. Chong, J. D. Joannopoulos, and M. Soljačić, *Phys. Rev. Lett.* **100**, 013905 (2008); *Nature (London)* **461**, 772 (2009); Z. Yu, G. Veronis, Z. Wang, and S. Fan, *Phys. Rev. Lett.* **100**, 023902 (2008); H. Takeda and S. John, *Phys. Rev. A* **78**, 023804 (2008); D. Han, Y. Lai, J. Zi, Z.-Q. Zhang, and C. T. Chan, *Phys. Rev. Lett.* **102**, 123904 (2009); X. Ao, Z. Lin, and C. T. Chan, *Phys. Rev. B* **80**, 033105 (2009); M. Onoda and T. Ochiai, *Phys. Rev. Lett.* **103**, 033903 (2009); T. Ochiai and M. Onoda, *Phys. Rev. B* **80**, 155103 (2009).

<sup>9</sup>S. L. Zhu, B. G. Wang, and L. M. Duan, *Phys. Rev. Lett.* **98**, 260402 (2007); B. Wunsch, F. Guinea, and F. Sols, *New J. Phys.* **10**, 103027 (2008); R. Shen, L. B. Shao, B. Wang, and D. Y. Xing, *Phys. Rev. B* **81**, 041410(R) (2010).

<sup>10</sup>Y. D. Chong, X. G. Wen, and M. Soljačić, *Phys. Rev. B* **77**, 235125 (2008).

<sup>11</sup>N. M. Litchinister, A. I. Maimistov, I. R. Gabitov, R. Z. Sagdeev, and V. M. Shalaev, *Opt. Lett.* **33**, 2350 (2008); L. G. Wang, Z.-G. Wang, J.-X. Zhang, S.-Y. Zhu, *ibid.* **34**, 1510 (2009); X. Chen, L. G. Wang, and C. F. Li, *Phys. Rev. A* **80**, 043839 (2009).

<sup>12</sup>S. Lim, C. Caloz, and T. Itoh, *IEEE Trans. Microwave Theory Tech.* **52**, 1142 (2004).

<sup>13</sup>F. Zhang, G. Houzet, E. Lheurette, D. Lippens, M. Chaubet, and X. Zhao, *J. Appl. Phys.* **103**, 084312 (2008).

<sup>14</sup>J. B. Pendry, A. J. Holden, D. J. Robbins, and W. J. Stewart, *IEEE Trans. Microwave Theory Tech.* **47**, 2075 (1999).

<sup>15</sup>J. B. Pendry, *Phys. Rev. Lett.* **85**, 3966 (2000).

<sup>16</sup>M. C. K. Wiltshire, J. B. Pendry, I. R. Young, D. J. Larkman, D. J. Gilderdale, and J. V. Hajnal, *Science* **291**, 849 (2001).

<sup>17</sup>D. Schurig, J. J. Mock, B. J. Justice, S. A. Cummer, J. B. Pendry, A. F. Starr, and D. R. Smith, *Science* **314**, 5801 (2006).

<sup>18</sup>N. I. Landy, S. Sajuyigbe, J. J. Mock, D. R. Smith, and W. J. Padilla, *Phys. Rev. Lett.* **100**, 207402 (2008).

<sup>19</sup>C. Rockstuhl, F. Lederer, C. Etrich, T. Pertsch, and T. Scharf, *Phys. Rev. Lett.* **99**, 017401 (2007).

<sup>20</sup>V. Yannopapas, *Opt. Commun.* **282**, 4152 (2009).

<sup>21</sup>R. B. Johnson and R. W. Christy, *Phys. Rev. B* **6**, 4370 (1972).

<sup>22</sup>V. Yannopapas, *Phys. Rev. B* **73**, 113108 (2006).

<sup>23</sup>I. Thanopoulos, E. Paspalakis, and V. Yannopapas, *Nanotechnology* **19**, 445202 (2008).

<sup>24</sup>N. Shalkevich, A. Shalkevich, L. Si-Ahmed, and T. Bürgi, *Phys. Chem. Chem. Phys.* **11**, 10175 (2009).

<sup>25</sup>S. Mühlig, C. Rockstuhl, V. Yannopapas, T. Bürgi, and F. Lederer, *Opt. Express* **19**, 9607 (2011).

<sup>26</sup>R. Sainidou, N. Stefanou, and A. Modinos, *Phys. Rev. B* **69**, 064301 (2004).

<sup>27</sup>N. Stefanou, V. Yannopapas, and A. Modinos, *Comput. Phys. Commun.* **113**, 49 (1998); **132**, 189 (2000).

<sup>28</sup>H. J. Lee, Q. Wu, and W. Park, *Opt. Lett.* **34**, 443 (2009).

<sup>29</sup>V. A. Tamma, J. H. Lee, Q. Wu, and W. Park, *Appl. Opt.* **49**, A11 (2010).

<sup>30</sup>A. Blanco, E. Chomski, S. Grabtchak, M. Ibisate, S. John, S. W. Leonard, C. Lopez, F. Meseguer, H. Miguez, J. P. Mondia, G. A. Ozin, O. Toader, and H. M. van Driel, *Nature (London)* **405**, 437 (2000).

<sup>31</sup>G. Frens, *Nature Phys. Sci.* **241**, 20 (1973).